



Indoor Radon Mapping and Assessment Excess Lifetime Cancer Risk in the Quarry Area of Shira, Bauchi State Nigeria

Auwalu Baballe^{1,2*} and S. A. Dalhatu²

¹Department of Physics, Faculty of science, Bauchi State University, Gadau, Bauchi State, Nigeria.

²NanoScience and Technology Research Group, Department of Physics, Bauchi State University, Gadau, Bauchi State, Nigeria.

³Federal University of Health Science, Azare, Nigeria.

Corresponding Author email: abuumusaab@gmail.com

ABSTRACT

The radioactive gas radon (Rn) is considered an indoor air pollutant due to its detrimental effects on human health. In fact, exposure to Rn is among the most important causes of lung cancer after tobacco smoke. The study aims to measure indoor radon concentration and evaluate the excess lifetime cancer risk from its exposure. The indoor radon concentrations were measured using electronic semiconductor detector (RAD7). The indoor radon activity concentration varies from 76.0 Bqm⁻³ to 217.4 Bqm⁻³ with a mean value of 149.3 Bqm⁻³. The result for Annual effective dose (E_{aed}) calculated from the measured indoor radon was 3.79 mSv/y, which are clearly above the permissible limit of 100 Bqm⁻³ and 1.15 mSv/y set by (WHO) and (UNSCEAR, 2000). The potential health risk was determined by computing Excess Lifetime Cancer Risk (ELCR) and lung cancer cases per year per million person (LCC). The map for the distribution and exposure rate due to indoor Radon for the study area was also plotted using Golden surfer 12 software. The average values for (ELCR) and (LCC) are respectively, 1.4×10^{-2} and 70.07 per millions, which is lower than the limit range of 170–230 per million persons recommended by ICRP. These measurements provide valuable insights for evaluating public radiation exposure and establishing robust radiological safety protocols.

Keywords: Indoor Radon, Annual effective dose, RAD7, lung cancer and Surfer software

INTRODUCTION

Radon is an imperceptible, naturally occurring radioactive gas emitting alpha radiation. It arises from the decay of ²²⁶Ra, a long-lived radionuclide with a 1600-year half-life, within the ²³⁸U radioactive decay series. ²²²Rn decays emit 5.49 MeV alpha particles, producing a series of radionuclides, primarily ²¹⁴Po and ²¹⁸Po, which contribute more than 90% of the total radiation dose associated with radon exposure [1]. The primary source of indoor radon is uranium, which is found in drinking water, building materials, and the rocks and soil beneath homes. Long-term exposure to high indoor radon concentrations can have pathological consequences and functional

respiratory alterations, raises the possibility of getting lung cancer [2]. Smoking is the sole factor surpassing radon as a leading cause of lung cancer. An estimated 10% of all lung cancer fatalities have been linked to prolonged inhalation of radon gas in enclosed spaces or open air [3]. Radon is generated by ²³⁸U decay in soil and bedrock. ²³⁸U distribution varies across geological formations, areas with high concentrations, such as granitic bedrock, tend to have elevated radon levels. Bedrock and soil with greater porosity and permeability allow ²²²Rn to escape more quickly into groundwater and the atmosphere, Radon gas poses a substantial health risk when it accumulates indoors, particularly in homes and workplaces [4]. Granite quarries emit



radioactive substances that contaminate the surrounding environment, affecting air, water, vegetation, and wildlife, and polluting soil and food crops [5].

Radon is the largest contributor to human radiation exposure, responsible for more than half of the global average annual dose. Regulatory actions and mitigation strategies are essential to address radon risks, necessitating comprehensive knowledge of radon levels and geographic distribution [6]. Countries worldwide have implemented Radon mapping techniques to identify areas of elevated exposure risk. The maps serve as essential tools for radon risk assessment and mitigation in housing development [7]. Several studies have revealed different techniques for identifying radon risks areas such as measurement of indoor radon concentration, radon concentration in soil gas and airborne surveys of gamma-ray [8]. Interpreting soil-gas radon data is challenging due to significant daily and seasonal fluctuations near the surface and localized variations over short distances [9]. Therefore, Researchers have developed sophisticated multivariate models, including regression kriging and machine learning algorithms, to predict radon levels. These models rely on indoor radon measurements as a key response variable [10]. Radon potential mapping has been conducted by indoor radon concentration measurements in many countries such as Ireland [11] and Belgium [12]. Integration of indoor radon measurements with geological

units enhances predictive modeling and spatial precision [13].

Ventilation rates and temperature variations are the key factors influencing indoor radon level fluctuations. Measuring indoor radon is vital, as it contributes significantly to the total natural radiation exposure, exceeding 50% of the overall dose [14]. Extensive research has been published recently on radon measurements worldwide and epidemiological investigations exploring the link between indoor radon exposure and lung cancer risk [15] and [16]. Existing literature indicates that no research has been conducted to assess the health risks from indoor radon exposure stemming from the granite quarry of the study area. The study intends to assess indoor radon concentrations and evaluate the excess lifetime cancer risk resulting from prolonged exposure.

MATERIAL AND METHODS

Study Area

The study area is located in the quarry site of Shira, Bauchi North, Nigeria as shown in figure 1, bounded by coordinates 11°30'15''N 10°1'2''E, covering a land area of 1,321 km² and a population density of 234,014. The region experiences a biphasic climate, comprising distinct dry and rainy seasons, with temperatures fluctuating between 23°C and 38°C. The underlying geology of Shira district consists of two main formations: the Tertiary Kerri-Kerri and granite (migmatite) geological units [17].

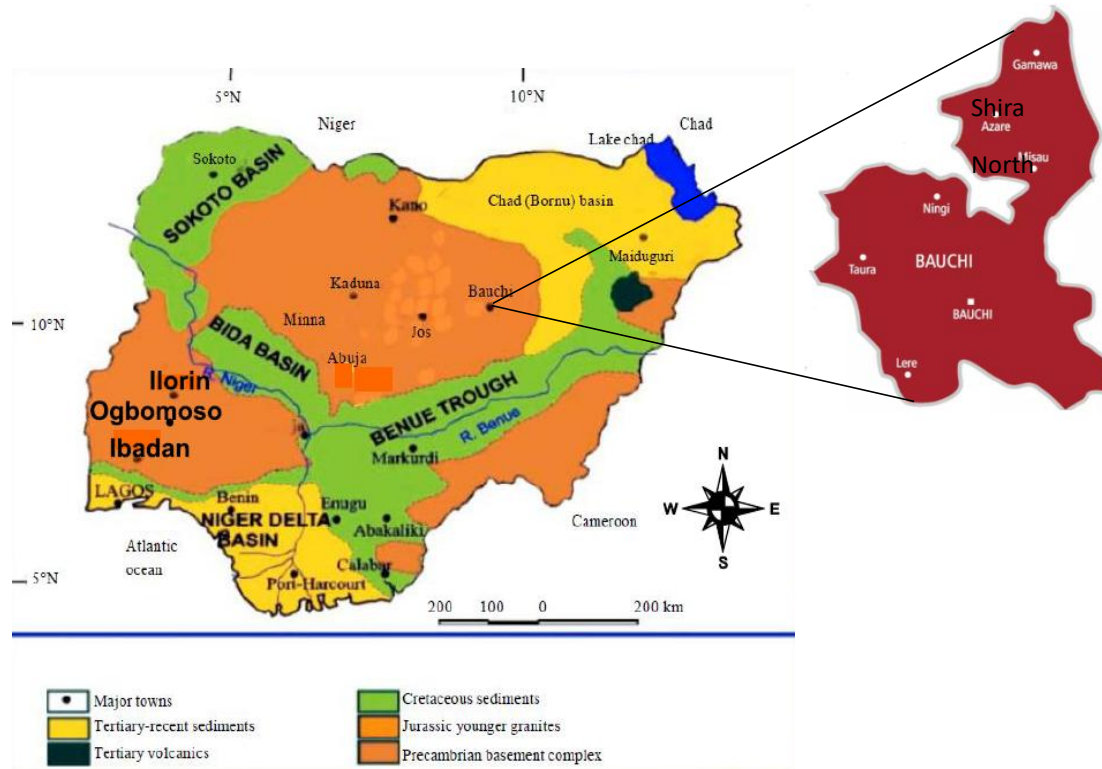


Figure 1: Map of the study area.

Indoor Radon Measurements

Indoor radon concentrations of ten residential houses near the Shira granite quarry area were determined using electronic semiconductor detector (RAD7), a specialized instrument developed for measurements of radon in any kind of air; indoor air, outdoor air, soil air and water. The advantage of RAD7 and the usage of a semiconductor detector is the energy resolution feature, if we consider the energies of ^{218}Po , ^{214}Po their separation is 1.68 MeV and the detector's energy resolution is about 100 keV. The decays from the two isotopes can clearly be separated. The RAD7 spectrum shows radon daughters, but not radon itself. And also, the technique has a tremendous advantage in sniffing or grab-sampling, very few instruments other than RAD7 are able to do the task [3].

To ensure accurate readings, the RAD-7 was connected to a calcium sulfate (CaSO_4)

desiccant and purged before each measurement, eliminating moisture and residual radon. The mean value for the indoor radon was obtained from 20 min cycle. Measurements were taken within a controlled temperature range (15-30 °C) and corrected for background radiation. The RAD-7 device ensured an absolute accuracy of $\pm 5\%$ [18].

RAD-7 Principle of Work

RAD7 is an instrument that converts alpha radiation from the decay of ^{222}Rn to electric signal. The RAD7 amplifies, filters and sorts the signal according to their strength. It's insensitive to beta and gamma radiation, so there will be no interference from beta-emitting gases or from gamma radiation fields. The radon concentration inside the RAD7 can be determined by the below differential equation.

$$\frac{dC(t)}{dt} = -\lambda C(t) \quad 1.0$$

$$\frac{dC_{po}(t)}{dt} = \lambda_{po}C(t) - \lambda_{po}C_{po}(t) \quad 1.1$$

$C(t)$: represents activity concentration of radon in the detector chamber, and λ its corresponding decay constant. Also $C_{po}(t)$ and λ_{po} denote the concentration and decay constant of polonium-218 respectively.

When air is pumping into RAD7, there will be a time when the radon concentration in the surrounding C_0 , will be equal to that of RAD7.

Therefore equation 3.2, becomes,

$$dC_{Po}(t) dt = \lambda_{Po}C_0 - \lambda_{Po}C_{Po}(t) \quad 1.3$$

by solving equation 3.3, and applying initial condition,

$$C_{Po}(t) = C_0 \quad 1.4$$

Activity concentration of Radon can be obtained from equation 3.4, which illustrates the theoretical operation of RAD7.

RESULTS AND DISCUSSION

Indoor Radon Concentration

The Indoor radon concentration of ten different location of Quarry area of Shira, Bauchi State Nigeria are presented in the Table 1. The data presents statistical summary values for radon concentration, including minimum, maximum, mean, and standard error. The activity concentration of the Indoor radon varies from $76.0 \pm 4.16 \text{ Bq/m}^3$ to $217.4 \pm 5.07 \text{ Bq/m}^3$ with a mean value of $149.29 \pm 4.59 \text{ Bq/m}^3$. Significant variability is observed in the measured data across different locations shown in the Fig. 1. The mean radon concentration is higher than the WHO recommended limits of 100 Bq/m^3 . The highest radon activity concentration is

$$\text{AED (mSv/y)} = C_{Rn} \times F \times T \times O \times \text{DCF} \quad 1.5$$

In the equation 1.5, C_{Rn} represents Indoor radon concentration (Bq/m^3), F is the

observed at the sampling location H8, that sample location is situated nearer to the quarry operations than all the other sampling locations. The higher value of indoor radon of this study which could be attributed to the quarry activities in the area. ^{222}Rn activity concentrations exhibit spatial variability due to differences in soil type, geology, topography and local meteorological conditions.

The study conducted in the Saudi Arabia, the findings suggest that relative humidity positively influences radon concentration, as increased moisture in the air reduces radon diffusion and traps it indoors [18]. In another study, the higher indoor radon can be attributed to Uranium and thorium content in the underlying earth, along with radon diffusion through soil and rock openings [19]. The concentrations of indoor radon and thoron are directly linked to the activity of ^{226}Ra and ^{232}Th in building materials, and indirectly influenced by soil composition and local geophysical characteristics which facilitates radon entry into dwellings [20]. Compared to previous studies, the mean activity indoor radon of the present study is higher than [21] and [22] reported, yet is comparably lower obtained in the previous by [23] and is in close agreement with findings of another study by [24].

Annual effective dose and Evaluation of cancer risk

The Radiological parameters such as annual effective dose (AED), Excess Lifetime Cancer Risk (ELCR) and lung cancer cases per year per million person (LCC) through Indoor radon exposure were computed using equations 1.5, 1.6 and 1.7 respectively.

equilibrium factor between radon and its daughters (0.4), O stands for occupancy factor

(0.8), T is the Number of hours in a year (8760 h/yr) and DCF is the dose conversion actor (9×10^{-6} mSv/hr per Bq/m³) [22]. The annual effective dose (AED) varies from 1.92 mSv/y to 5.13 mSv/y with a mean value of 3.76 mSv/y as tabulated on Table 1, Our findings

indicate an average annual effective dose that is higher than the worldwide average of 1.15 mSv/y set by [25]. The results is in agreement with that reported by [18] and [21].

The Excess Lifetime Cancer Risk is given by,

$$ELCR = AED \times DL \times RF \quad 1.6$$

Table 1: Indoor radon concentration, annual effective dose (AED), Excess Lifetime Cancer Risk (ELCR) and lung cancer cases per year per million person (LCC)

Location code	Indoor radon concentration (Bq/m ³)	Annual effective dose AED (mSv/y)	Excess Lifetime Cancer Risk (ELCR)	lung cancer cases per year per million person (LCC)
H1	137.3 ± 4.12	3.46	1.3×10^{-2}	62.28
H2	178.9 ± 5.23	4.51	1.7×10^{-2}	81.18
H3	86.8 ± 4.06	2.19	8.4×10^{-3}	39.42
H4	141.0 ± 3.91	3.55	1.4×10^{-2}	63.90
H5	167.6 ± 5.45	4.22	1.6×10^{-2}	75.96
H6	203.5 ± 6.43	5.13	1.9×10^{-2}	115.74
H7	92.1 ± 3.79	2.32	8.9×10^{-3}	41.76
H8	217.4 ± 5.07	5.48	2.1×10^{-2}	98.64
H9	76.0 ± 4.16	1.92	7.4×10^{-3}	34.56
H10	192.3 ± 3.72	4.85	1.8×10^{-2}	87.30
average	149.29 ± 4.59	3.76	1.4×10^{-2}	70.07

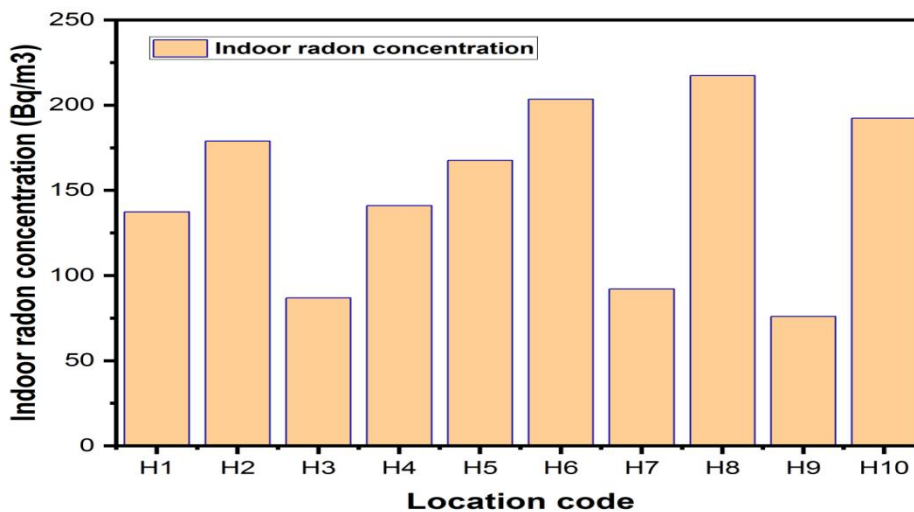


Figure 2: Variation Indoor radon concentration across different locations

AED stands for the annual effective dose, DL is the average duration lifetime (70 years) and RF is the cancer risk factor ($RF = 0.05 \text{ Sv}^{-1}$)

[26]. The Excess Lifetime Cancer Risk (ELCR) range from 1.3×10^{-2} to 8.9×10^{-3} with an average value of 1.4×10^{-2} .

Lung cancer cases per million people per year are calculated, based on a risk factor of 18

$\times 10^{-6}$ cases per million people per millisievert of radiation exposure [27].

$$LCC = DL \times 18 \times 10^{-6} \quad 1.7$$

lung cancer cases per year per million person (LCC) through Indoor radon exposure was computed to varies from 34.56 per million to 115.74 per million with a mean value 70.07 per million. The average (ELCR) and (LCC) were 1.4×10^{-2} and 70.07 per million, respectively, falling below the recommended limit of 170-230 cases per million persons set by the International Commission on Radiological Protection (ICRP) [28].

Indoor radon Mapping

The spatial distribution of indoor radon exposure rates is depicted in Figure 3, resulting from the integration of measurement data and geographic coordinates using Surfer 12 software for spatial analysis and mapping. Surfer 12 software facilitated the mapping of the study area and guided the selection of sampling points according to geological formation features. The contour maps depicted locations that are likely prone to an increase indoor radon exposure [29].

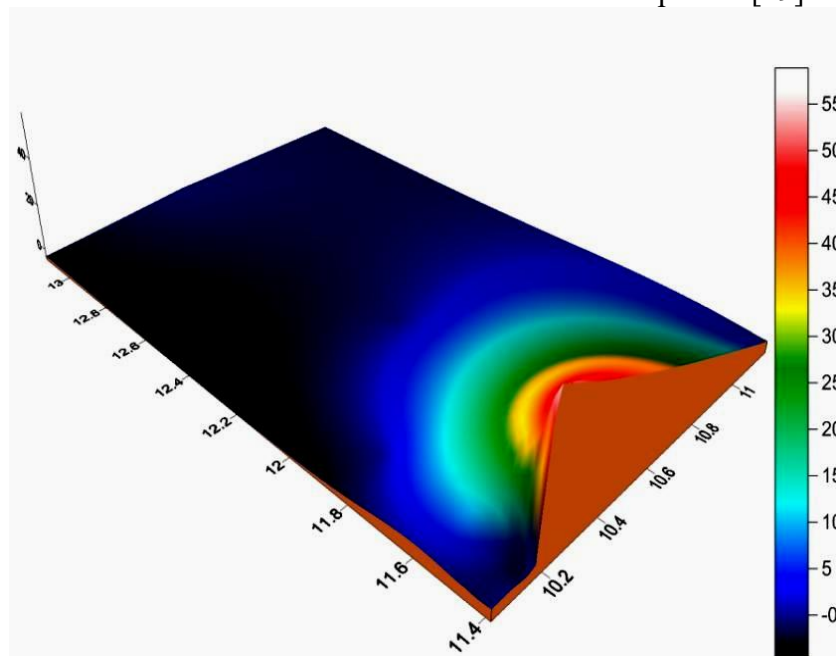


Figure 3: Contour map for Indoor radon of the study area.

The Barnett model [30] was applied to categorize Indoor radon concentrations into three distinct index categories: low, medium, and high. Figure 3 illustrates the spatial distribution of radon indices, categorizing regions into low (less than 30 kBq/m³), medium (30-100 kBq/m³), and high (exceeding 100 kBq/m³) radon levels [31].

Based on the radon contour map plotted for the study area, The highest radon activity concentration is observed at the sampling location H8, which is represents by dark red on the countour map. Granite intracrustal rocks forms the primary geological foundation of the region. The the sampling location H9

has the lowest radon activity concentration which is represents by blue colour on the map.

CONCLUSION

The research aims to quantify indoor radon exposure and estimate the resultant lifetime cancer risk, enabling a comprehensive risk assessment. Indoor radon activity concentrations ranged from 76.0 ± 4.16 Bq/m³ to 217.4 ± 5.07 Bq/m³, with a mean concentration of 149.29 ± 4.59 Bq/m³. Radon concentrations exceed WHO guidelines, with an average value higher than the recommended 100 Bq/m³. The calculated Effective Lung Cancer Risk (ELCR) and Lung Cancer Cases (LCC) were 1.4×10^{-2} and 70.07 per million, respectively, well below the ICRP's recommended threshold of 170-230 cases per million. The radiological assessment reveals that quarrying in the study area does not poses a significant health risk to the community from the radiation exposure. A visual representation of indoor Radon distribution and exposure rates was generated for the study area using Golden Surfer 12. However, prolonged exposure to even relatively low and moderate levels of radon increases the risk of developing lung cancer. The created radon map will facilitate proactive planning and decision-making for radon mitigation strategies. As enshrined in the WHO guidelines, the nigerian government should establish a national refrence level for radon concentration to as serve as public awareness about the health risk from its long-term exposure.

Acknowledgement

The research is funded by Tertiary Education Trust Fund (TETFund) through institutional based research approved 2024 for Bauchi State University, Gadau Nigeria.

REFERENCES

1. Mihci, M., et al., *Indoor and outdoor Radon concentration measurements in Sivas, Turkey, in comparison with geological setting*. Journal of environmental radioactivity, 2010. 101(11): p. 952-957.
2. Torres-Durán, M., et al., *Residential radon and lung cancer in never smokers. A systematic review*. Cancer letters, 2014. 345(1): p. 21-26.
3. Abuelhia, E., *Evaluation of annual effective dose from indoor radon concentration in Eastern Province, Dammam, Saudi Arabia*. Radiation Physics and Chemistry, 2017. 140: p. 137-140.
4. Berens, A.S., et al., *The use of gamma-survey measurements to better understand radon potential in urban areas*. Science of the total environment, 2017. 607: p. 888-899.
5. Dalhatu, S.A., et al., *Radiation hazard assessment of natural radionuclides in the soil samples from the quarry area of Shira, Bauchi State, Nigeria*. BIMA JOURNAL OF SCIENCE AND TECHNOLOGY (2536-6041), 2024. 8(2A): p. 342-350.
6. Haruna, R., et al., *Assessment of geogenic radon potential in Johor Malaysia*. Journal of Radioanalytical and Nuclear Chemistry, 2020. 326: p. 1065-1074.
7. Kemski, J., et al., *From radon hazard to risk prediction-based on geological maps, soil gas and indoor measurements in Germany*. Environmental Geology, 2009. 56: p. 1269-1279.
8. Ptiček Siročić, A., et al., *Short-term measurement of indoor radon concentration in Northern Croatia*. Applied Sciences, 2020. 10(7): p. 2341.



9. Appleton, J., *Radon: sources, health risks, and hazard mapping*. Ambio, 2007: p. 85-89.
10. Coletti, C., et al., *The assessment of local geological factors for the construction of a Geogenic Radon Potential map using regression kriging. A case study from the Euganean Hills volcanic district (Italy)*. Science of The Total Environment, 2022. 808: p. 152064.
11. Dubois, G., *An overview of radon surveys in Europe Report EUR21892*. EC, Office for Official Publications of the European Communities, Luxembourg, 2005.
12. Cinelli, G., *Indoor and outdoor natural radioactivity in the vulsini volcanic district (central Italy): estimation of doses and radiological risks*. 2012.
13. Miles, J. and K. Ball, *Mapping radon-prone areas using house radon data and geological boundaries*. Environment International, 1996. 22: p. 779-782.
14. Maghraby, A.M., K. Alzimami, and M. Abo-Elmagd, *Estimation of the residential radon levels and the population annual effective dose in dwellings of Al-kharj, Saudi Arabia*. Journal of Radiation Research and Applied Sciences, 2014. 7(4): p. 577-582.
15. Sheen, S., et al., *An updated review of case-control studies of lung cancer and indoor radon-Is indoor radon the risk factor for lung cancer?* Annals of occupational and environmental medicine, 2016. 28: p. 1-9.
16. Sherafat, S., et al., *First indoor radon mapping and assessment excess lifetime cancer risk in Iran*. MethodsX, 2019. 6: p. 2205-2216.
17. Ibrahim, S., et al., *Terrestrial gamma radiation dose (TGRD) levels in northern zone of Bauchi, Nigeria: mapping and statistical relationship between gamma dose rates and geological formations*. Gadau Journal of Pure and Allied Sciences, 2023. 2(1): p. 9-15.
18. Yousef, A. and K. Zimami, *Indoor radon levels, influencing factors and annual effective doses in dwellings of Al-Kharj City, Saudi Arabia*. Journal of Radiation Research and Applied Sciences, 2019. 12(1): p. 460-467.
19. Mehra, R. and P. Bala, *Estimation of annual effective dose due to radon level in indoor air and soil gas in Hamirpur district of Himachal Pradesh*. Journal of Geochemical Exploration, 2014. 142: p. 16-20.
20. Adelikhah, M., et al., *Radiological assessment of indoor radon and thoron concentrations and indoor radon map of dwellings in Mashhad, Iran*. International Journal of Environmental Research and Public Health, 2021. 18(1): p. 141.
21. Khan, F., et al., *Study of indoor radon concentrations and associated health risks in the five districts of Hazara division, Pakistan*. Journal of Environmental Monitoring, 2012. 14(11): p. 3015-3023.
22. Tezcan, F., S. Aközcan, and S. Özden, *Indoor radon (^{222}Rn) measurements and assessment of human risk in the dwellings of Edirne (Türkiye)*. Journal of Radioanalytical and Nuclear Chemistry, 2023. 332(11): p. 4629-4640.
23. Clouvas, A., S. Xanthos, and G. Takoudis, *Indoor radon levels in Greek schools*. Journal of environmental radioactivity, 2011. 102(9): p. 881-885.
24. Venoso, G., et al., *Radon concentrations in schools of the*



25. Neapolitan area. Radiation measurements, 2009. 44(1): p. 127-130.
26. UNSCEAR, *Sources, effects and risks of ionizing radiation, united nations scientific committee on the effects of atomic radiation (UNSCEAR) 2016 report: report to the general assembly, with scientific annexes*. 2000: United Nations.
27. Isinkaye, M. and H. Emelue, *Natural radioactivity measurements and evaluation of radiological hazards in sediment of Oguta Lake, South East Nigeria*. Journal of Radiation Research and Applied Sciences, 2015. 8(3): p. 459-469.
28. Azhdarpoor, A., et al., *Assessment of excess lifetime cancer risk and risk of lung cancer due to exposure to radon in a middle eastern city in Iran*. Radiation Medicine and Protection, 2021. 2(03): p. 112-116.
29. Hoffman, F.O., *Lung cancer risk from radon and progeny and statement on radon*. ICRP publication 115, Ann. ICRP 40 (1). 2012, Oxford University Press.
30. Esan, D.T., et al., *Determination of residential soil gas radon risk indices over the lithological units of a Southwestern Nigeria University*. Scientific Reports, 2020. 10(1): p. 7368.
31. Barnet, I., et al., *Radon in geological environment—Czech experience Czech Geological Survey Special Papers*. 2008.
32. Ajiboye, Y., M. Isinkaye, and M. Khanderkar, *Spatial distribution mapping and radiological hazard assessment of groundwater and soil gas radon in Ekiti State, Southwest Nigeria*. Environmental earth sciences, 2018. 77: p. 1-15.